Comparative Medicine
Copyright 2012
by the American Association for Laboratory Animal Science

Vol 62, No 2
April 2012
Pages 99–108

Original Research

A New Apparatus and Surgical Technique for the Dual Perfusion of Human Tumor Xenografts in Situ in Nude Rats

Robert T Dauchy,* Erin M Dauchy, Lulu Mao, Victoria P Belancio, Steven M Hill, and David E Blask

We present a new perfusion system and surgical technique for simultaneous perfusion of 2 tissue-isolated human cancer xenografts in nude rats by using donor blood that preserves a continuous flow. Adult, athymic nude rats (Hsd:RH-*Foxn1^{rnu}*) were implanted with HeLa human cervical or HT29 colon adenocarcinomas and grown as tissue-isolated xenografts. When tumors reached an estimated weight of 5 to 6 g, rats were prepared for perfusion with donor blood and arteriovenous measurements. The surgical procedure required approximately 20 min to complete for each tumor, and tumors were perfused for a period of 150 min. Results showed that tumor venous blood flow, glucose uptake, lactic acid release, O_2 uptake and CO_2 production, uptake of total fatty acid and linoleic acid and conversion to the mitogen 13-HODE, cAMP levels, and activation of several marker kinases were all well within the normal physiologic, metabolic, and signaling parameters characteristic of individually perfused xenografts. This new perfusion system and technique reduced procedure time by more than 50%. These findings demonstrate that 2 human tumors can be perfused simultaneously in situ or ex vivo by using either rodent or human blood and suggest that the system may also be adapted for use in the dual perfusion of other organs. Advantages of this dual perfusion technique include decreased anesthesia time, decreased surgical manipulation, and increased efficiency, thereby potentially reducing the numbers of laboratory animals required for scientific investigations.

Abbreviations: AKT, serine–threonine protein kinase; EGFR, epithelial growth factor receptor; ERK1/2, extracellular signal regulated kinase p44/46; GSK3β, glycogen synthase kinase 3β; LA, linoleic acid; G protein, guanine nucleotide binding protein; MEK, mitogen-activated protein kinase kinase; TFA, total fatty acids.

Traditional models of organ perfusion used techniques and strategies that often involved the interruption of blood flow from the host to the tissue under investigation for some intermittent period of time.[17,25,32,33] This interruption resulted in periods of anoxia, hypoxia, and nutrient deprivation leading to significant, and often irreversible, damage to organ metabolism and physiology. In the mid-1980s, our laboratory used a unique tissue-isolated rodent tumor model[40] to develop a perfusion system and technique[13] that sustained a continuous blood supply to the tumor throughout the procedure. This perfusion model avoided many of these pitfalls, particularly in regard to continuous blood supply and was subsequently used successfully in a variety of investigations involving both normal and neoplastic tissue physiology, metabolism, and proliferation.[2-11,13,35-40] Most recently, we used this perfusion model to investigate the circadian regulation of molecular endocrine, dietary, and metabolic signaling pathways of human cancers by the circadian neurohormone melatonin,[29,30] and the disruptive effects of environmental light at night.[2,4,5,11,12,39,40] We found that tissue-isolated MCF7 steroid-negative human breast cancer xenografts perfused in situ with blood from human subjects exposed to light at night had greater tumor growth and metabolism due to inhibition of normal nocturnal melatonin levels.[2] This effect occurred through a cAMP-dependent, inhibitory-G-protein–coupled, MT_1 melatonin receptor-mediated signal transduction pathway. These investigations prompted our development of a new system that was easy to use and reduced experimental time and numbers of animals.

Here we describe a new rapid-delivery dual-perfusion system apparatus and methodology that accommodates simultaneous investigation of 2 tissue-isolated human tumor xenografts yet decreases perfusate delivery time. We coupled this dual-perfusion methodology with our earlier method for growing tissue-isolated human tumor xenografts in nude rats for perfusion in situ,[2,3] which was based on our initial system.[13,36] Because of this combined technology, we were able to simultaneously examine the metabolism and physiology of 2 of the most widely studied human cancers, HeLa cervical carcinoma and HT29 colorectal adenocarcinoma. We investigated glucose and total fatty acid (TFA) uptake, O_2 consumption, CO_2 and lactate production, tumor cAMP production, signal transduction and transcriptional regulation events, and proliferative responses. This novel system and technique greatly improves our ability to study fundamental

Received: 07 Oct 2011. Revision requested: 02 Nov 2011. Accepted: 10 Nov 2011.
Department of Structural and Cellular Biology, Tulane University School of Medicine, Tulane, Louisiana.
Corresponding author. Email: rdauchy@tulane.edu

http://prime-pdf-watermark.prime-prod.pubfactory.com/ | 2025-02-25

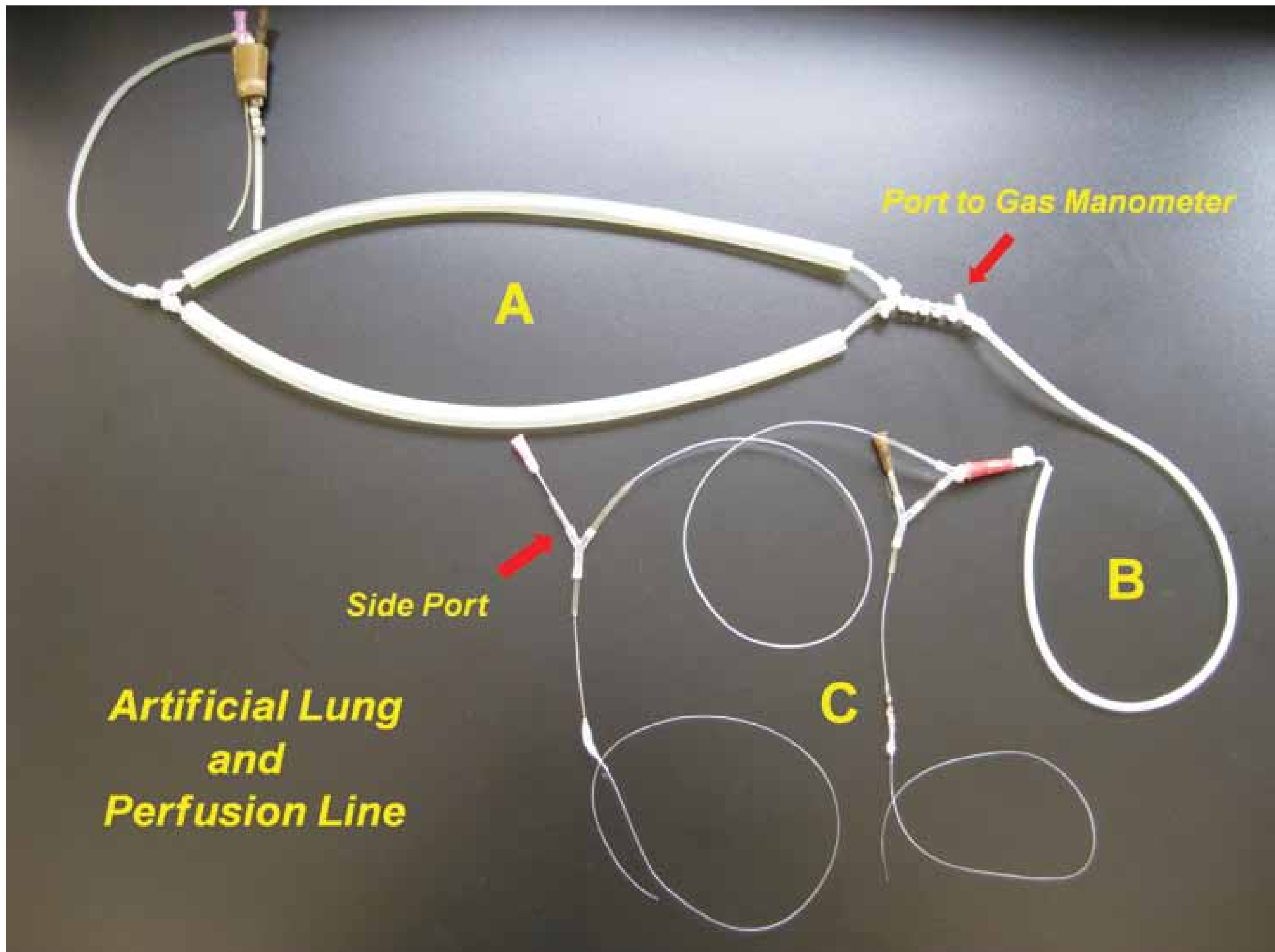

Figure 1. Photo of artificial lung and perfusion line apparatus used for dual perfusion of tissue-isolated HeLa human cervical and HT29 human colorectal adenocarcinoma xenografts. Peristaltic transducer unit (A) for peristaltic pump head leading from reservoir to artificial lung (B) and dual perfusion catheters with side ports (C) leading to tumor xenografts.

metabolic, physiologic, and proliferative characteristics in diverse human tumors in vivo and may be useful in the perfusion and investigation of various normal organ systems.

Materials and Methods

Reagents. HPLC-grade chloroform, ethyl ether, methanol, glacial acetic acid, heptane, hexane, and Sep-Pak C18 cartridges for HPLC extraction of samples were purchased from Fisher Chemical (Pittsburgh, PA). Free fatty acid, cholesterol ester, triglyceride, phospholipid, and rapeseed oil methyl ester standards, as well as boron trifluoride–methanol, potassium chloride, sodium chloride, and perchloric and trichloroacetic acids were purchased from Sigma Scientific (St Louis, MO). The HPLC standards, (±) 5-HETE (catalog no. 34210) and 13(S)-HODE (catalog no. 38610), and ultrapure water (catalog no. 400000) were purchased from Cayman Chemical (Ann Arbor, MI).

Animals, housing conditions, facility modifications and improvements, and diet. The female and male athymic nude mice (Hsd:athymic nude-*Foxn1*^{nu}) and adult, homozygous, athymic, inbred nude rats (Hsd:RH-*Foxn1*^{rnu}), 3 to 4 wk of age, used in this study were purchased from Harlan (Indianapolis, IN). These SPF animals were maintained in environmentally controlled rooms (25 °C; humidity, 50% to 55%) with a 12:12-h light:dark cycle (lights on 0600; 125 lx; 304 µW/cm^2). Animal rooms were lighted with a series of 3 overhead ballast–lamp systems containing 4 cool-white fluorescent lamps each (F32T8TL741, Alto Collection 32W, Philips, Somerset, NJ); fluorescent lamps used in the 24-h-illuminated corridors were identical; animal rooms were completely devoid of light-at-night contamination during the dark phase. To ensure that all animals remained infection-free from both bacterial and viral agents, serum samples from sentinel animals were tested quarterly and during the course of this study by using immunoassays (Multiplex Fluorescent Immunoassay 2, Research Animal Diagnostic Laboratory, Columbia, MO; rats: rat coronavirus, Sendai virus, pneumonia virus of mice, sialodacryoadenitis virus, Kilham rat virus, Toolan H1 virus, reovirus type 3, *Mycoplasma pulmoni*, lymphocytic choriomeningitis virus, mouse adenovirus 1 and 2, Hantaan virus, *Encephalitozoon cuniculi*, cilia-associated

http://prime-pdf-watermark.prime-prod.pubfactory.com/ | 2025-02-25

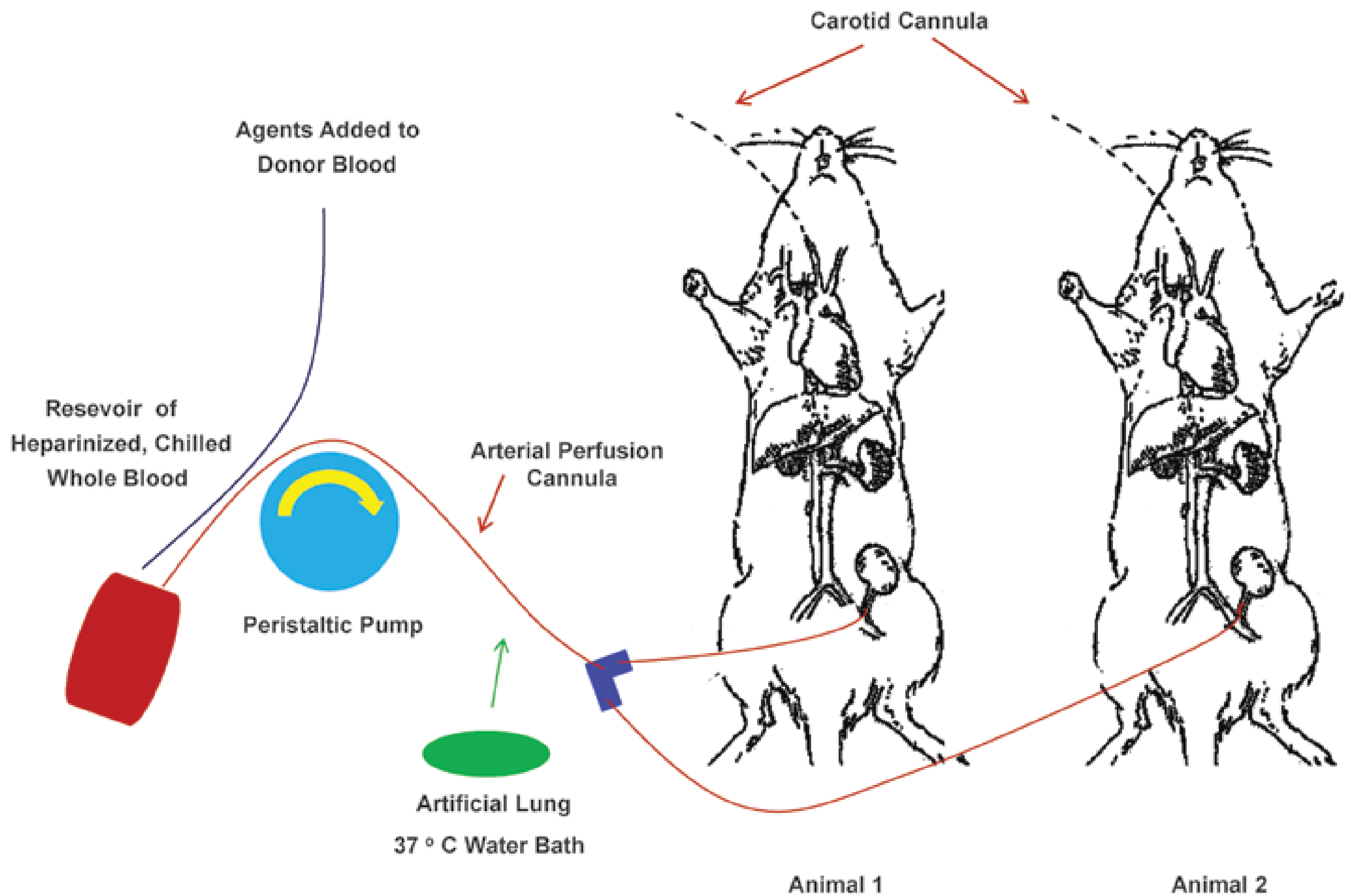

Figure 2. Schematic diagram of the artificial lung and dual perfusion system for perfusing tissue-isolated HeLa human cervical and HT29 human colorectal adenocarcinoma xenografts in situ with donor rat blood. The arterial blood collected from donor rats just prior to perfusions was placed in a plastic reservoir in ice and gently stirred with a magnetic stirrer. The peristaltic pump courses the arterial blood through the artificial lung that was immersed in a water bath at 37 °C. As the tumors received the fresh arterial blood from the reservoir by means of the perfusion system, tumor venous blood drained from the infusion catheter and was collected in a preweighed vial on ice. Each tumor rested undisturbed in the warmed environment of the body of the rat.

respiratory bacillus, parvovirus NS1, rat parvoviruses, and rat murine virus, and rat theilovirus; Mice: mice minute virus, mouse parvovirus types 1 through 3, Theiler murine encephalomyelitis virus, epizootic diarrhea of infant mice, Sendai virus, *Mycoplasma pulmoni*, mouse hepatitis virus, parainfluenza virus, reovirus type 3, lactate dehydrogenase-elevating virus, ectromelia virus, murine adenovirus types 1 and 2, polyomavirus, *Encephalitozoon cuniculi*, cilia-associated respiratory bacillus, *Clostridium piliforme*, mouse cytomegalovirus, K virus, Hantaan virus, mammalian orthoreovirus serotype 3, mouse pneumonia virus, and mouse thymic virus). Animals were given free access to food (Purina 5053 Irradiated Laboratory Rodent Diet, Purina Mills, Washington, DC), prepared in accordance with national standards,[27] and acidified water. Quadruplicate evaluations of this diet indicated that it contained 4.1 g TFA per 100 g of diet, composed of 0.03% myristic (C14:0), 12.53% palmitic (C16:0), 0.22% palmitoleic (C16:1n7), 3.15% stearic (C18:0), 21.78% oleic (C18:1n9), 56.48% linoleic (C18:2n6), 5.28% γ-linolenic, and 0.26% arachidonic (C20:4n6) acids. Minor amounts of other fatty acids comprised 0.27%. Conjugated linoleic acids and trans-fatty acids were not found. Over 90% of the TFA was in the form of triglycerides; more than 5% was in the form of free fatty acids. Animals were maintained in an AAALAC-accredited facility in accordance with *The Guide for the Care and Use of Laboratory Animals*.[21] All procedures for animal use were approved by the Tulane University IACUC.

Tumor xenograft implantation, growth, and histopathology. Originally, human cervical-derived HeLa and colorectal-derived HT29 cells were obtained from the American Type Culture Collection (catalog nos. CCL2 and HTB38, respectively; Manassas, VA) and cultured in our laboratory. Prior to inoculation for tumor growth, the injection sites of all mice were cleaned with 70% isopropanol, treated with povidone–iodine (catalog no. VMDS093917, Medline, Mundelein, IL), rinsed with warm sterile water, and allowed to dry. By using a 1-mL syringe with a 22-gauge needle (Becton–Dickinson, Franklin Lakes, NJ), 1×10^7 HeLa human cervical cancer cells or HT29 human colorectal cells in 0.1 mL culture media were inoculated subcutaneously on the flank immediately caudal to the right axilla in female (HeLa) or male (HT29) mice, respectively, and the tumors grew as solid masses. All procedures were conducted in a biologic safety cabinet by using aseptic techniques (gloves, masks, and so forth).

http://prime-pdf-watermark.prime-prod.pubfactory.com/ | 2025-02-25

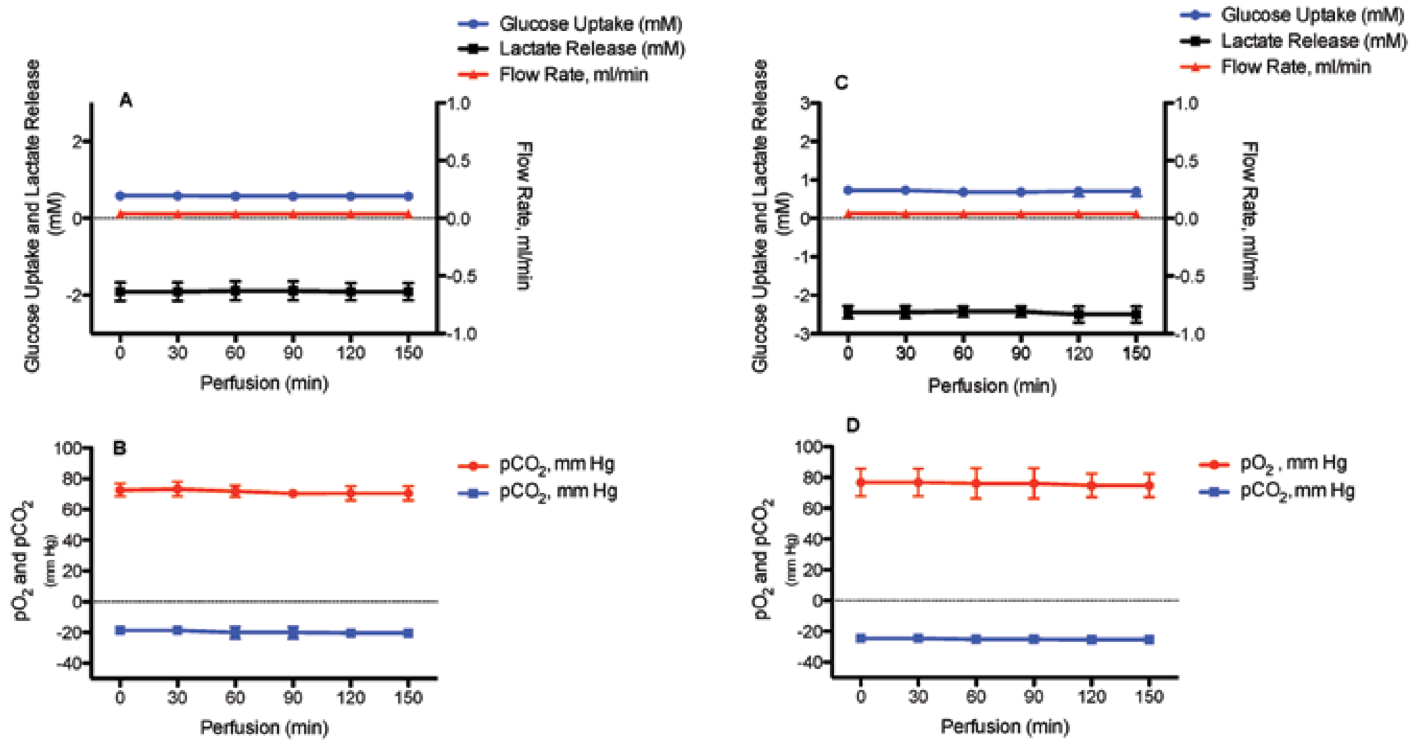

Figure 3. The effects of arterial blood perfusion through the artificial lung and dual perfusion system on flow rate, glucose uptake, lactate release, pO_2 uptake, and pCO_2 release across tissue-isolated HeLa human cervical and HT29 human colorectal adenocarcioma xenografts perfused in situ. Tumor perfusions were 150 min each; values are expressed as mean ± 1 SD (*n* = 4 per time point).

When the tumors reached approximately 1.5 g, the mice were euthanized by CO_2 narcosis, and the tumors were excised and placed in ice-cold saline for subsequent establishing of tissue-isolated tumors in nude rats.[2,5-11,35,36,38-40] Briefly, rats were anesthetized lightly by using ketamine (89.1 mg/kg IP)–xylazine (9.9 mg/kg IP) solution (MWI Veterinary Supply, Meridian, IN) delivered through a 25-gauge, 5/8-in. tuberculin syringe and prepped for an aseptic surgical procedure. A 3-mm cube of tumor was sutured with 5-0 black braided silk suture (Ethicon, Somerville, NJ) to the tip of a vascular stalk formed from the ligated caudal superficial epigastric artery and vein. The subcutaneous implant was enclosed in a sterile paraffin-film envelope and inserted into the inguinal fossa. The skin incision was closed with 4-0 suture (Dexon S, Sherwood Davis and Geck, St Louis, MO). Rats recovered from anesthesia approximately 45 min after this surgical procedure. Before recovery from surgery, each rat received a single dose of buprenorphine (0.1 mg/kg SC; MWI Veterinary Supply, Meridian, IN) through a tuberculin syringe; additional doses were provided as needed in response to signs of distress. In addition, ophthalmic lubricant was applied to eyes of the rats to help prevent eye irritation and cornea drying.

The human cancer xenografts grew as subcutaneous implants. The xenograft vascular supply was limited to new vessels connected to the inguinal artery and vein. Latency to a detectable tumor mass (that is, from day of implantation to day of first palpable, pea-size mass) and growth were measured for each rat used in each of the perfusion experiments.[40] Growth rates (g per day) were generated by linear regression analysis from the estimated tumor weights during the course of this study, and final tumor weights were determined by weighing at the end of each experiment. The HT29 human colorectal adenocarcinoma xenografts were histopathologically confirmed highly differentiated grade I colorectal adenocarcinoma tumors, and the HeLa human cervical adenocarcinoma xenografts were histopathologically confirmed to be poorly differentiated, high grade masses. When tumors reached approximately 5 to 7 g, they were prepared for the in situ perfusion procedure.

Collection of arterial blood from donor rats. Prior to initiation of the dual tumor perfusions, 3 to 4 adult nude female (for HeLa) or male (for HT29) rats were anesthetized by using ketamine–xylazine solution (89.1 mg/kg and 9.9 mg/kg IP). Animals were heparinized by jugular injection of sodium heparin (25 mg/kg; Sagent Pharmaceuticals, Schaumburg, IL). Arterial blood (40 to 50 mL) was collected by catheter from the right carotid artery of donor rats (for 2 perfusions), pooled, filtered through a 2-in. × 2-in. cheesecloth pad (Kendall Curity Gauze Sponge; Tyco Healthcare, Mansfield, MA), stored in a reservoir under mineral oil (catalog no. M1180-500ML, Sigma Scientific) and chilled at 4 °C in a reservoir on ice and gently mixed by using a mechanical stirrer (model no. 6975-171; Corning, Corning, NY).

Artificial lung and dual perfusion system. The new 'artificial lung' and dual-perfusion system (Figure 1) is composed of 3 single-line components in one: a peristaltic transducer assembly unit for the pump head, leading from the reservoir and coupling to the artificial lung, and the modified dual-perfusion catheters (inner diameter, 0.28 mm; outer diameter, 0.61 mm; polyethylene

http://prime-pdf-watermark.prime-prod.pubfactory.com/ | 2025-02-25

Table 1. Tumor glucose uptake, lactate release, and arterial and tumor venous oxygen and carbon dioxide levels in HeLa cervical and HT29 colon cancer xenografts that were perfused for 150 min with rodent donor blood in situ

	Glucose uptake		Lactate release	pO_2 (mm Hg)		pCO_2 (mm Hg)		pH	
	nmol/min/g	% of arterial supply	(nmol/min/g)	Artery	Vein	Artery	Vein	Artery	Vein
HeLa	11.4 ± 0.9	(16.2 ± 1.1%)	−20.4 ± 2.2	151.7 ± 2.7	80.9 ± 3.7[a]	33.2 ± 1.9	52.5 ± 2.0[a]	7.43 ± 0.02	7.32 ± 0.01[a]
HT29	14.5 ± 3.4	(18.7 ± 1.3%)	−28.0 ± 2.1	153.8 ± 1.8	77.8 ± 6.7[a]	31.3 ± 1.2	56.4 ± 1.1[a]	7.45 ± 0.01	7.32 ± 0.01[a]

[a]$P < 0.05$ compared with arterial value.

Table 2. Effects of perfusion of tissue-isolated HeLa cervical and HT29 colon adenocarcinoma xenografts

	Tumor weight (g)	cAMP (nmol/g tissue)	Total fatty acid uptake (µg/min/g)	LA uptake (µg/min/g)	13-HODE (ng/min/g)		[³H]thymidine incorporation (dpm/µg DNA)	DNA content (mg/g)
					Arterial supply	Venous output		
HeLa xenografts (*n* = 4)	5.9 + 0.3	0.29 ± 0.01	2.47 ± 0.44	0.71 ± 0.08	not detectable	0.352 ± 0.07	21.2 ± 0.6	2.5 ± 0.1
HT29 xenografts (*n* = 4)	5.5 ± 0.5	0.41 ± 0.03[a]	3.06 ± 0.47[a]	0.86 ± 0.08[a]	not detectable	3.23 ± 0.81[a]	25.9 ± 1.6[a]	2.7 ± 0.1

[a]$P < 0.05$ compared with value for HeLa cervical cancer xenografts.

10; catalog no. 427401, Clay Adams Intramedic, Sparks, MD). The transducer consists of 2 silicone tubes (length, 0.3 m; inner diameter, 1.35 mm; outer diameter, 3.35 mm; catalog no. 80-1065-91, Amersham Pharmacia Biotech, Piscataway, NJ) located inside 2 larger silicone tubes (inner diameter, 6.34 mm; outer diameter, 10 mm; catalog no. 241631; Dow Corning, Midland, MI), which were seated on either side of the pump head of the peristaltic pump (model no. 1205, Harvard Instruments, Natick, MA). The artificial lung consists of medical-grade silastic tubing (length, 0.30 m; inner diameter, 0.76 mm; outer diameter, 1.65 mm; catalog no. 602-235; Dow Corning) contained within silicone tubing (length, 0.30 m; inner diameter, 2.38 mm; outer diameter, 3.97 mm; catalog no. 06411-63; Cole Parmer Instrument, Vernon Hills, IL). Polypropylene Y connectors and side ports (inner diameter, 3.2 mm; length, 23 mm; catalog no. 15-320-10A, Fisher Scientific) were used to join the 3 single-line components. The inner silastic tube void volume (0.170 mL), containing the blood perfusate, was permeable to the surrounding atmospheric gases within the exterior, nonpermeable silicone tubing line. The gas phase, containing a mixture of air and 5% CO_2 saturated in water at 37 °C, was adjusted to physiologic conditions by using a dual-flow gas proportioner (series no. 2942, MG Industries, Valley Forge, PA). All gas components were adjusted to maintain arterial pO_2 at 155 mm Hg, pCO_2 at 33 mm Hg, and pH at 7.40. The peristaltic pump settings were adjusted to provide normal venous flow rates of approximately 0.115 and 0.125 mL/min for the HeLa and HT29 tissue-isolated xenografts, respectively, as determined at the initiation of each experiment (Figure 2). The artificial lung and perfusion line void volume was 0.650 mL (reservoir to tumors); at a flow rate of 0.130 mL/min, blood flow travel time from reservoir to tumors was 5.00 min.

When tumors reached 5 to 7 g in estimated weight, rats were prepared for arterial and venous cannulation for tumor assessment between 0600 and 0700. Initially, the 2 host tumor-bearing rats were anesthetized as described earlier and placed side-by-side on the operating table on a heating pad, with overlying heat lamps to maintain normal body temperature and with the rats' heads toward the surgeon. In a sequential manner, first rat 1 and then rat 2 were prepped for the surgery. A dissecting microscope (catalog no. 22-2000, CM-III, Mentor O and O, South Shore Park, Hingham, MA), modified for ease of movement over the surgical fields, was used throughout the procedures. Beginning with rat 1, the right common carotid artery was exposed and cannulated with a 4-in. length of PE50 tubing (inner diameter, 0.58 mm; outer diameter, 0.96 mm; catalog no. 427411, Clay Adams Intramedic) and attached to a syringe (23-gauge needle; Precision Glide, Becton Dickinson) containing 0.1 mL sodium heparin (1000 U/mL). Body core temperature was maintained at 37 °C and monitored and measured continuously by rectal probe and telethermometer (model no. 47, Yellow Springs Instrument, Yellow Springs, OH). Respiration and body temperature were observed at frequent intervals and recorded.

Both rats then were rotated 180° in this supine position to allow access to the posterior epigastric region. A small (2 cm) incision was made at the site of the tumor, and the skin over the inguinal fossa region was removed by retractors. The human tumor tissue and femoral vascular tree were exposed, cleaned, and then covered with a 1-in × 1-in. gauze pad (Kendall Curity Gauze Sponge) soaked with warm saline, to prevent cooling and drying of the tissue. The femoral artery and vein were separated and cleaned on both the proximal (left) and distal (right) sides of the epigastric stalk. Three 2-in. lengths of 5-0 black braided-silk suture (catalog no. 640G, Ethicon, Somerville, NJ) were coursed around both the proximal femoral artery and vein, and two 2-in. lengths were coursed separately around the distal artery and vein. The wound site then was covered with a 2-in. × 2-in. gauze pad.

The dissecting microscope was repositioned over rat 2 in the adjacent surgical field, and both the carotid arterial catheter insertion and tumor vascular preparatory procedure in the inguinal fossa region were repeated. Both rats then were heparinized by the previously inserted carotid catheter (0.1 mL, 1000 U/mL). Without repositioning of the microscope, the proximal portion of the femoral tumor vein of rat 2 was secured by ligature and slightly retracted, whereas the tumor vein 0.5 cm distal to the retracted site and proximal to the epigastric stalk was cannulated with a winged infusion set (25 gauge × 1/2 in., catalog no. CE0197, Terumo) that was modified so that the needle tip is bent at a 90° angle for ease of insertion, and the cannula was secured by 2 ligatures. The femoral vein distal to the epigastric stalk was closed off by ligature, ensuring that all venous blood flow drained from the tissue-isolated tumor only. The femoral artery proximal to the epigastric stalk was ligated and slightly retracted for ease of access. The proximal femoral artery was nicked and the perfusion catheter inserted (beveled end facing the tumor) and secured by

http://prime-pdf-watermark.prime-prod.pubfactory.com/ | 2025-02-25

Table 3. Fatty acid and lipid contents (μg/g) of HeLa cervical and HT29 colon adenocarcinomas

	HeLa					HT29				
Fatty acid	Triglycerides	Phospholipids	Free fatty acids	Cholesterol esters	Total	Triglycerides	Phospholipids	Free fatty acids	Cholesterol esters	Total
C14:0	54 ± 7	17 ± 2	2 ± 1	6 ± 2	78 ± 3	43 ± 12	22 ± 4	3 ± 1	7 ± 2	74 ± 16
C16:0	431 ± 22	246 ± 12	100 ± 3	10 ± 2	785 ± 31	465 ± 24	244 ± 40	67 ± 3	8 ± 2	803 ± 66
C16:1	37 ± 15	61 ± 3	2 ± 1	10 ± 2	103 ± 21	64 ± 3	61 ± 10	3 ± 1	10 ± 3	137 ± 14
C18:0	305 ± 115	198 ± 13	129 ± 13	11 ± 2	642 ± 28	164 ± 13	238 ± 48	100 ± 8	7 ± 1	554 ± 81
C18:1	361 ± 26	144 ± 13	39 ± 5	12 ± 1	549 ± 26[a]	734 ± 42	223 ± 75	51 ± 10	9 ± 1	1016 ± 106
C18:2	583 ± 23	216 ± 34	78 ± 4	9 ± 1	887 ± 80[a]	937 ± 50	270 ± 88	61 ± 11	7 ± 2	1274 ± 131
C20:4	142 ± 8	464 ± 6	48 ± 5	21 ± 3	675 ± 12	70 ± 15	487 ± 94	37 ± 9	21 ± 3	608 ± 119
Total	1983 ± 148[a]	1332 ± 39	400 ± 46	78 ± 6	3793 ± 206[a]	2466 ± 199	1571 ± 310	318 ± 18	70 ± 4	4453 ± 471

[a]$P < 0.05$ compared with value for HT 29 human colon cancer xenografts.

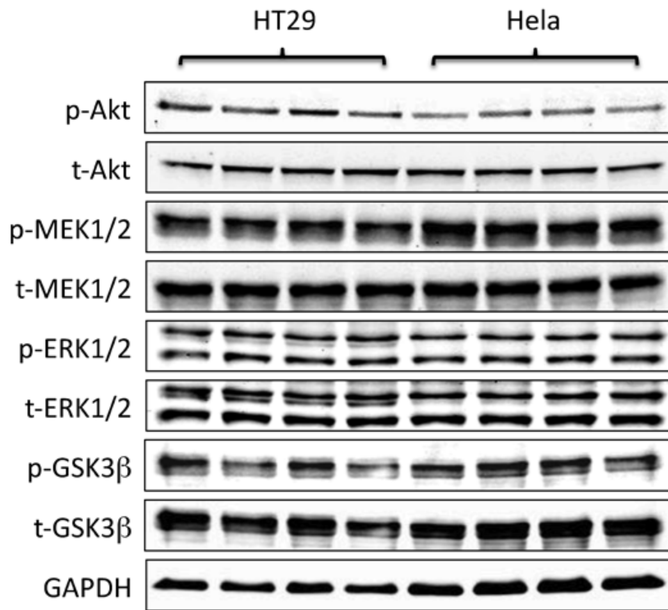

Figure 4. Western blot analyses for the expression of the nonphosphorylated (t) and phosphorylated (p) forms of Akt, MEK 1/2, ERK 1/2 (p44/p42), and GSK3β in HT29 human colorectal (left lanes) and HeLA human cervical (right lanes) adenocarcinomas in vivo harvested after 150 min of perfusion with donor nude rat blood. GADPH is shown as a loading control. Each lane depicts bands from a single tumor.

2 ligatures; during this part of the procedure, the tumor received oxygenated blood by reverse reflux flow through the distal femoral artery and collateral branches. Finally, the femoral artery distal to the epigastric stalk is closed off by using ligature. The rat was exsanguinated through the carotid catheter, ensuring that the tumor was completely isolated from the host and receiving fresh donor arterial blood by the reservoir and perfusion system only and draining through the tumor venous cannula only. Beginning at time 0 min and approximately every 30 min thereafter, arterial and venous blood samples were collected until conclusion of the 150-min perfusion.

Once perfusion was established in rat 2, the dissecting microscope was repositioned over rat 1 and the tumor arterial and venous catheterization procedure was repeated. In addition, once the perfusion pump was engaged for whole-blood perfusion of the tumor in rat 2, the machine was not turned off, even during subsequent catheterization of the epigastric artery leading to the tumor of rat 1. Blood flow from both catheters occurred simultaneously and continuously during the course of the 150-min perfusions. Incorporation of [^{3}H]thymidine into tumor DNA was initiated 20 min prior to the end of each experiment by injecting 20 μL of physiologic saline containing [methyl-^{3}H]thymidine (2 μCi per gram estimated tumor weight; catalog no. NET027005MC, New England Nuclear, Perkin Elmer, Boston, MA) into the arterial catheter (Figure 1, side port). At the completion of each study, tumors were freeze-clamped under liquid nitrogen, weighed, and stored at −85 °C until analysis. At the end of the experiment, the lumen of the artificial lung and perfusion line was disinfected by perfusing for 20 min with 10% bleach solution (Clorox, Oakland, CA) followed by 20 min with 0.9% sterile saline (Baxter Healthcare, Deerfield, IL).

Measurement of tumor xenograft arteriovenous acid–gas, glucose, and lactate measurements. During the course of these perfusions, arterial and venous whole blood samples were taken for measurements of pH, pO_2, pCO_2, glucose uptake and lactate production, and hematocrit by using a handheld Analyzer (iSTAT1 with CG4+ and CG8+ cartridges, Abbott Laboratories, East Windsor, NJ). Utilization of glucose and production of lactate were calculated from arteriovenous differences (in nmol/g) multiplied by the blood flow rate (in mL/min).

Fatty acid extraction and analysis, tumor 13-HODE production, and determination of tumor cAMP levels. Arterial plasma TFA were extracted from 0.1-mL arterial and venous samples after addition of heptadecanoic acid (C17:0), as described previously.[2-11,13,37,38] Tumor tissue TFA and linoleic levels in HeLa human cervical and HT29 human colorectal tumors (n = 4 per group) were extracted from 0.1 mL of 20% tissue homogenate, as previously described.[2,7-13,35-37] Tumor TFA and fatty acid lipid fractions, that is, triglycerides, phospholipids, free fatty acids, and cholesterol esters were separated by using silica gel G plates (catalog no. 01011, Uniplate, Alltech, Newark, DE), as described previously.[7-13,35,39]

http://prime-pdf-watermark.prime-prod.pubfactory.com/ | 2025-02-25

Analyses were performed in duplicate. Methyl esters of the fatty acids were analyzed by using a gas chromatograph (model no. HP 5890A, Hewlett–Packard, Palo Alto, CA) equipped with a fused-silica capillary column (30 m × 0.25 mm [inner diameter]; film thickness, 0.25 µm; catalog no. 2330, Supelco, Bellefonte, PA), as described previously.[7-13,35,39] Values for total fatty acids (TFA) represent the sum of the 7 major fatty acids (myristic, palmitic, palmitoleic, stearic, oleic, linoleic, and arachidonic acids) present in blood plasma as free fatty acids, cholesterol esters, triglycerides, and phospholipids as well as other plasma lipids. Physiologic levels of TFA in different batches of donor arterial blood collected from fed rats differed by as much as 10%. Analyses showed this variation altered the rate of TFA and linoleic acid (LA) uptake tumor somewhat but not the rate of uptake as a percentage of supply to the tumor, which remained consistent at about 16% and 19% for HeLa human cervical and HT29 human colorectal adenocarcinoma xenografts, respectively. Rates of TFA and LA uptake are presented here for statistical comparisons as both absolute values and as percentage of supply. Tumor production of 13-HODE was measured as previously described, by using 0.2-mL arterial and venous plasma samples.[2,5,6,10,35,39,40] Tumor levels of cAMP were determined by ELISA assay (GE Lifesciences, Piscataway, NJ) as described previously.[2,9,12]

Western blot measurement of tumor phosphorylated kinases. Frozen tumor tissue was ground into fine powder and lysed in Tissue Extraction Reagent I (catalog no. FN0071, Invitrogen, Camarillo, CA) containing Tris (50 mM, pH 7.4), EDTA (20 mM), NP40 (0.5%), NaCl (150 mM), PMSF (0.3 mM), NaF (1 mM), $NaVO_4$ (1 mM), dithiothreitol (1 mM), with protease and phosphatase inhibitor cocktails (protein:inhibitor, 100:1[v/v]) and homogenized by using a Potter–Elvehjem homogenizer (Wheaton Science Products, Millville, NJ). The tissue lysates were centrifuged for 10 min at 10,000 × *g*, 4 °C. Protein concentrations of the supernatants were determined by using a kit (Bio-Rad, Hercules, CA).[5,10] Total protein (90 µg per sample) was separated electrophoretically on a 12% denaturing polyacrylamide gel and electroblotted (Hybond, GE Healthcare). After incubation with 5% nonfat milk in Tris-buffered saline containing 0.05% Tween, the immunoblots were probed with antibodies to phosphorylated extracellular signal-regulated kinase p44/42 (ERK 1/2; (Thr202/Tyr204), phosphorylated mitogen-activated protein kinase kinase (MEK1/2; Ser217/221), phosphorylated serine–threonine protein kinase (AKT; Ser473), or phosphoGSK3β (Ser9; Cell Signaling, Beverly, MA). The same blots were stripped and reprobed with antibodies to AKT, p44/42 ERK1/2, MEK1/2, or GSK3β (Cell Signaling), respectively. GAPDH was used as the loading control (Millipore, Billerica, MA). The bands were visualized and quantified by using the Odyssey Infrared Imaging System and Odyssey Software (Licor Biosciences, Lincoln, NE).

Statistical analysis. All data are presented as mean ± 1 SD and compared by using one-way ANOVA followed by the Student–Neuman–Keul posthoc test. Differences among group means were considered statistically significant at a P value less than 0.05.

Results

Tumor growth rates. For both HeLa and HT29 tumors, latency-to-onset of detectable tumor growth was recorded and tumor weights were estimated every other day. Consistent with previous results, growth rates depended on the type of tumor and strain of the rat.[2-7,10] Latency-to-onset of tumor growth for HeLa and HT29 adenocarcinomas were consistently 8 and 12 d, respectively, and tumor growth rates were 0.09 ± 0.01 and 0.12 ± 0.01 g/d, respectively. At the time of perfusion, the mean body weight of adult female nude rats was 246.5 ± 16.7 g and that of male rats was 348.5 ± 15.8 g, with corresponding tumor burden (tumor weight divided by body weight, %) of 2.4% ± 0.1% and 1.5% ± 0.1%, respectively; both percentages are well below values that are known to lead to metabolic disruption and cachexia[16,26] in rodents and that might compromise results.

Observations during steady-state hemodynamics and measurement of tumor arteriovenous differences. Spontaneous changes (typically decreases) in blood flow rate sometimes occur during the course of perfusion studies and may alter nutrient uptake and release.[4,6,8,13,24,35,36,38-40] Because of this possibility, changes in blood flow must be minimized. Within each tumor group (n = 4 per group), whole-blood acid–gas analysis, arterial and venous hematocrits, and tumor venous flow rate fluctuated less than 2% during the course of the 150-min perfusions (Figure 3). At the constant arterial flow rate used in the current study, the time required for blood flow from reservoir to the 2 tumors (5.00 min) represented a 60% improvement over that for the previous single-perfusion system.[6,13] As a result, the data represent the combined values for the 4 perfusions of each tumor group. Arterial and venous hematocrits were 43.8% ± 1.5% and 45.7 ± 1.5%, respectively, for HeLa tumors and 44.4% ± 1.5% and 46.4 ± 1.5%, respectively, for HT29 xenografts. These values indicate less than 5% hemoconcentration of the blood as it passes through the tumors. Flow rates for the HeLa and HT29 tumor xenografts were 0.114 ± 0.002 and 0.124 ± 0.003 mL/min, respectively. Similarly, arteriovenous difference measurements for glucose, lactate, pO_2, and pCO_2, which tend to vary in parallel with flow rate,[7,37,38] were constant throughout the course of all perfusions. Mean arteriovenous glucose and lactate concentrations for the HeLa xenografts were 5.92 ± 0.01 and 5.16 ± 0.02 mM, respectively, and for HT29 xenografts were 1.17 ± 0.07 and 3.35 ± 0.03 mM, respectively. Because of these effects, the perfused tumor was considered to be in a steady state if 30 min passed with less than a 5% change occurred in blood flow or if a reversible change occurred that had minimal effects on nutrient uptake or release. These criteria were applied to the data summarized in Tables 1 through 3.

Glucose uptake and lactate release, pH, pO_2, and pCO_2 in both tumor types are shown in Table 1. Arterial pO_2 saturation of the HeLa and HT29 adenocarcinomas (99.4% ± 0.2% and 99.5% ± 0.2%, respectively) remained constant throughout the course of the perfusions. Uptake of glucose and lactate release was slightly higher ($P < 0.05$) in HT29 (27.2%) than HeLa (39.2%) xenografts. This difference corresponded to 17.0% greater ($P < 0.05$) O_2 consumption and 17.1% greater ($P < 0.05$) CO_2 release in HT29 than HeLa adenocarcinoma xenografts, reflecting the slightly higher metabolic rate of the colorectal cancer tissue. Arterial and venous pH remained constant and similar during both sets of perfusions for the HeLa and HT29 adenocarcinoma xenografts.

Table 2 details the final HeLa and HT29 perfused tumor cAMP content, TFA and LA uptakes, 13-HODE release, [^{3}H]thymidine incorporation into tumor DNA, and DNA content. cAMP levels in perfused HeLa tumor xenografts were nearly 30% lower ($P < 0.05$) than those in HT29 xenografts. In addition, protein content differed significantly ($P < 0.05$) between HeLa (3.21 ± 0.31 µg/µL) and HT29 (4.41 ± 0.51 µg/µL) xenografts. Tumor TFA and LA uptake by the perfused HeLa adenocarcinomas differed significantly

http://prime-pdf-watermark.prime-prod.pubfactory.com/ | 2025-02-25

($P < 0.05$) from that of the HT29 adenocarcinomas. TFA and LA uptake by HeLa xenografts represented 14.3% ± 1.6% and 14.6% ± 2.1%, respectively, of the arterial supply to the tumor, compared with 18.1% ± 2.6% and 20.0 ±1.6%, respectively, for the HT29 tumors. Tumor 13-HODE release by the HeLa adenocarcinomas was approximately 10% of that of the HT29 adenocarcinoma xenografts ($P < 0.05$).

The [^{3}H]thymidine made one pass through the tumor; unincorporated [^{3}H]thymidine appeared in the tumor blood 1 min after injection (0.22% ± 0.01% of total unincorporated; $n = 8$), reached a peak at 2 to 4 min (92.5% ± 1.8%) and was completely eliminated from the tumor venous blood in 15 min. Reflecting tumor metabolic and proliferative activity, incorporation of [^{3}H]thymidine into tumor DNA was about 24% lower ($P < 0.05$) in HeLa compared with HT29 adenocarcinomas. There was no significant difference in DNA content between the 2 tumors.

Fatty acid and lipid content of HeLa and HT29 human cancer xenografts. The TFA contents and lipid fractions of HeLa cervical and HT29 colorectal human adenocarcinomas are listed in Table 3. As shown, levels of the 7 major fatty acids comprising TFA were significantly ($P < 0.05$) higher in HT29 colorectal compared with HeLa cervical cancers. Linoleic acid (C18:2), the principal tumor-growth-stimulatory FA,[35,36,38] was in greatest abundance (HT29, 23.4% ± 0.4%; HeLa, 28.6% ± 0.3%), followed by palmitic and oleic acids and corresponding well with the proportional increase found the arterial blood plasma.

Western blot analysis of tumor phosphorylated kinases. Western blot analysis of the perfused HeLa and HT29 adenocarcinoma xenografts (Figure 4) demonstrated that expression of phosphorylated and total ERK 1/2, MEK, AKT, and GS3Kβ was robust and correlated well with tumor 13-HODE release rates and [^{3}H]thymidine incorporation into tumor DNA (Table 2).

Discussion

The purpose of the current study was to test a new dual-perfusion system and surgical technique for simultaneous perfusion of 2 different human cancer xenografts, namely, HeLa cervical and HT29 human colorectal adenocarcinomas, in nude rats in situ. The new 'artificial lung' and dual-perfusion system is a major innovation over the original single-perfusion system[13] developed in our laboratory in 1985 in terms of improved design and size, function, versatility, and ease of use.[13,36] Improvements of the new perfusion system, compared with the earlier version,[13, 36] include: 1) reduction in overall line length from 1.95 m (original system) to 0.9 m; (2) decrease in peristaltic transducer diameter and length (reduced from 0.75 m to 0.28 m); (3) decrease in catheter tubing dimensions; and, (4) insertion of the Y-coupling unit with second catheter; and (5) overall reduction in void volume from reservoir to tumor (1.2 mL to 0.65 mL). In addition, the methodology for preparing and perfusing the 2 tumors is quite different, in terms of timing of events (that is, anesthesia, surgical manipulations, initiation of perfusions and blood collections and acid–gas analysis), than that used in the single-perfusion system. The sequence and timing of the surgical steps in the overall procedure was critical, subsequently minimizing overlap and delays while providing sufficient time for the experimental arteriovenous blood collections during the simultaneous dual-perfusion procedure. This methodology also ensured that the operator had the time required for preparation of additional study animal**s** (rats 3, 4, and so forth) for entry into the perfusion scheme.

This novel system and procedure, using rodent donor whole-blood perfusates, was used to examine rapid changes in FA transport and the metabolism, physiology, and activation of signal transductions pathways leading to growth and proliferation of these 2 human cancers in vivo. This information cannot be obtained by using standard in vitro cell culture methods or other subcutaneous tumor models, leading to our use of the human cancer xenograft in situ as the experimental model.[13] Key advantages of our new system and methodology include: (1) decreased perfusate delivery time to the 2 tumors simultaneously; (2) minimal alterations in normal physiology and metabolism, due to the continuous, uninterrupted blood flow to both tumors simultaneously; (3) prompt assessment of kinetics of rapid growth responses; (4) minimal manipulation of the tissues with the current in situ methodology, as compared with the inherent additional manipulation and time factors necessary for ex situ procedures); (5) greater quality and quantity of tests that can be conducted concurrently; (6) improved quality of experimental results because of lack of cessation of blood flow to tumor tissue, which leads to prolonged anoxia and nutrient deprivation; (7) use of whole-blood perfusates (as for the single-tissue perfusion system[13,36]) to better maintain the normal metabolic and physiologic conditions in the host animal and tumor tissues,[2,4-12,35-39] as compared with the use of artificial, synthetic perfusates and ex situ excision methodologies common in other tissue perfusion experiments;[1,15,17,22-24,28,32,33,41] and, (8) potential considerable decrease in animal numbers, because one rat can be used for 2 tissue perfusions simultaneously, with an associated decreased chance for experimental error.

Great care must be taken during the course of the procedure to prevent vascular leakage and cessation of blood flow. All ligatures must be secured and the catheters and tumors manipulated as little as possible. With this caution in mind, the total time for surgical preparation of each tumor remained less than 20 min, with an overall success rate of 100%. Our results showed that steady-state hemodynamics were established within the first 10 min after initiation of perfusion and was sustained throughout the 150-min dual perfusion procedure, dramatically curtailing the time required for 2 individual tumor perfusions. Arterial and venous blood pH, pO_2, pCO_2, O_2 saturation, glucose and lactate concentrations, and arteriovenous differences for both the HeLa and HT29 human adenocarcinomas remained remarkably constant throughout the course of every perfusion. The arteriovenous difference measurements across each tumor type revealed a marked uptake of O_2 and output of CO_2 with constant flow rates and hematocrit values, demonstrating active and unimpeded tumor basal metabolism.

The first "tissue-isolated" tumor model was developed in the early 1960s by injecting mammary cancer cells into rat ovaries.[17,18] When the tumor–ovary tissue, with a single artery and vein, reached the defined size, it was excised and placed ex vivo in a perfusion chamber for the study of vascular and metabolic parameters. Other early investigators[1,25,28,32,33] and several recent studies[19,22-24,28,41] used perfusion techniques that focused on organ or tissue manipulation and removal from the host animal, causing cessation of blood flow to the tissue for extended periods of time during the procedure. The rapid whole-blood collection and measurement procedure used in the current study, coupled with a recent tissue-isolated model,[40] enables investigators to mea-

http://prime-pdf-watermark.prime-prod.pubfactory.com/ | 2025-02-25

sure immediate changes in basal metabolism and FA transport in vivo.

Wicha and colleagues[42] were the first to show in vitro that LA stimulates the incorporation of [^{3}H]thymidine incorporation into acid-precipitable material, a measure of enhanced proliferation, in normal mammary epithelial and tumor cells within 3 h after addition. Subsequently, LA was shown to be the principal growth-stimulatory fatty acid in rodent hepatoma tumors in vivo.[35,38] LA, an ω6 polyunsaturated fatty acid and the principal FA of the Western diet[14,34] and, interestingly, most laboratory animal chows, is converted to the mitogenic agent 13-HODE.[38] Levels of LA in these diets greatly exceed normal essential FA cellular requirements for growth (greater than 1% of total calories).[31] In our previous investigations using the original tissue-isolated tumor perfusion model, we determined that the uptake of LA and TFA and the formation of 13-HODE is in these human tumors is dependent on tumor cAMP levels.[2,3,7,10] We demonstrated growth stimulatory effects of LA in vivo in a number of human tumors including MCF7 steroid-positive and -negative breast,[2] head, and neck cancers[10] and leiomyosarcomas,[7] and in vitro in normal breast epithelium cells.[20] LA's oncogenic effects are diverse and related to its ability to upregulate the expression of a variety of genes and proteins involved in cell-cycle progression and survival and G-protein signaling (such as EGFR, MEK1/2, ERK1/2, and AKT) and the activation of GSK3β, a key respiratory gene involved in energy metabolism. The data provided here strongly support the active functioning of similar pathways in the HeLa cervical and HT29 colorectal human adenocarcinomas.

Currently we are using this dual-perfusion system to expand our studies relating to the influence of the circadian timing system (via melatonin) and its disruption (via light at night) on tumor growth and metabolism in laboratory animals and humans. We believe that this novel, rapid-delivery dual-perfusion system and methodology can easily be adapted to other normal and neoplastic tissues and may help provide insights into nutrient uptake and metabolism as they pertain to cancer, cachexia, and obesity-related diseases.

Acknowledgments

This work was supported in part by a Tulane University School of Medicine and Louisiana Cancer Research Consortium Startup Grant (no. 631455 to DEB), NIH grant (no. P20RR02020152), and the American Association for Laboratory Animal Science Grants for Laboratory Animal Science (GLAS) Award (to RTD). VPB is supported by P20RR020152 (NIH), NIA 5K01AG030074-02 (NIA), and The Ellison Medical Foundation New Scholar in Aging award 547305G1.

References

1. **Berger M, Haag LA, Goodman M, Ruerman NB.** 1976. Glucose metabolism in perfused skeletal muscle. Biochem J **158:**191–202.
2. **Blask DE, Brainard GC, Dauchy RT, Hanifin JP, Davidson LK, Krause JA, Sauer LA, Rivera-Bermudez MA, Dubocovich ML, Jasser SA, Lynch DT, Rollag MD, Zalatan F.** 2005. Melatonin-depleted blood from premenopausal women exposed to light at night stimulates growth of human breast cancer xenografts in nude rats. Cancer Res **65:**11174–11184.
3. **Blask DE, Dauchy RT, Sauer LA, Holowachuk E, Ruhoff M, Kopff H.** 1999. Melatonin inhibition of cancer growth in vivo involves suppression of tumor fatty acid metabolism receptor-mediated signal transduction events. Cancer Res **59:**4693–4701.
4. **Blask DE, Dauchy RT, Sauer LA, Krause JA, Brainard GC.** 2003. Growth and fatty acid metabolism of human breast cancer (MCF7) xenografts in nude rats: impact of constant light-induced nocturnal melatonin suppression. Breast Cancer Res Treat **79:**313–320.
5. **Blask DE, Hill SM, Dauchy RT, Xiang S, Yuan L, Duplessis T, Mao L, Dauchy E, Sauer LA.** 2011. Circadian regulation of molecular, dietary and metabolic signaling mechanisms of human breast cancer growth by the nocturnal melatonin signal and the consequences of its disruption by light at night. J Pineal Res **51:**259–269.
6. **Dauchy EM, Dauchy RT, Sauer LA, Davidson LK, Krause JA, Blue L, Lynch DT, Blask DE.** 2006. Human breast cancer xenografts perfused in situ in rats with growth-inhibitory agents: a new perfusion system that minimizes delivery time. J Am Assoc Lab Anim Sci **45:**38–44.
7. **Dauchy RT, Blask DE, Dauchy EM, Davidson LK, Tirrell PC, Greene MW, Tirrell RP, Hill CR, Sauer LA.** 2009. Antineoplastic effects of melatonin on a rare malignancy of mesenchymal origin: melatonin receptor-mediated inhibition of signal transduction, linoleic acid metabolism and growth in tissue-isolated human leiomyosarcomas xenografts. J Pineal Res **47:**32–42.
8. **Dauchy RT, Blask DE, Sauer LA.** 2000. Preparation of the inguinal fat pad for perfusion in situ in the rat: a surgical technique that preserves continuous blood flow. Contemp Top Lab Anim Sci **39:**29–33.
9. **Dauchy, RT, Blask DE, Sauer, LA, Davidson LK, Krause JA, Smith LC, Dauchy EM.** 2003. Physiologic melatonin concentration, ω3 fatty acids, and conjugated linoleic acid inhibit fatty acid transport in rodent hind limb skeletal muscle in vivo. Comp Med **53:**186–190.
10. **Dauchy RT, Dauchy EM, Davidson LK, Krause JA, Lynch DT, Tirrell PC, Tirrell RP, Sauer LA, Van der Riet P, Blask DE.** 2007. Inhibition of fatty acid transport and proliferative activity in tissue-isolated human squamous cell cancer xenografts perfused in situ with melatonin, eicosapentaenoic or conjugated linoleic acids. Comp Med **57:**377–382.
11. **Dauchy RT, Dauchy EM, Tirrell RP, Hill CR, Davidson LK, Greene MW, Wu J, Sauer LA, Blask DE.** 2010. Dark-phase light contamination disrupts circadian rhythms in plasma measures of physiology and metabolism. Comp Med **60:**348–356.
12. **Dauchy RT, Dupepe LM, Ooms TG, Dauchy EM, Hill CR, Mao L, Belancio VP, Slakey LM, Hill SM, Blask DE.** 2011. Eliminating animal facility light-at-night contamination and its effect on circadian regulation of rodent physiology, tumor growth, and metabolism: a challenge in the relocation of a cancer research laboratory. J Am Assoc Lab Anim Sci **50:**326–336.
13. **Dauchy RT, Sauer LA.** 1986. Preparation of 'tissue-isolated' rat tumors for perfusion: a new surgical technique that preserves continuous blood flow. Lab Anim Sci **36:**678–681.
14. **Dolecek TA, Grandits G.** 1991.Dietary polyunsaturated fatty acids and mortality in the Multiple Risk Factor Intervention Trial (MRFIT). World Rev Nutr Diet **66:**205–216.
15. **Gores GJ, Kost LJ, Larusso NF.** 1986. The isolated perfused rat liver: conceptual and practical considerations. Hepatology **6:**511–517.
16. **Gorselink M, Vaessen SF, van der Rlier LG, Leenders I, Kegler D, Caldenhoven E.** 2006. Mass-dependent decline of skeletal muscle function in cancer cachexia. Muscle Nerve **33:**691–693.
17. **Guillino PM.** 1968. In vitro perfusion of tumors, p 877–898. In: Norman JC, editor. Organ perfusion and preservation. New York (NY): Appleton–Century–Crofts.
18. **Guillino PM, Grantham FH.** 1961. Studies on the exchange of fluids between host and tumor. I. A method for growing "tissue-isolated" tumors in laboratory animals. J Natl Can Inst **27:**679–693.
19. **Hoy AJ, Peoples GE, McLennan PL.** 2009. The effect of vasoconstrictors on oxygen consumption in testing and contracting skeletal muscle of the autologous pump-perfused rat hindlimb. J Physiol Pharmacol **60:**155–160.
20. **Hill SM, Blask DE, Xiang S, Yuan L, Mao L, Dauchy RT, Dauchy EM, Frasch T, Duplesis T.** 2011. Melatonin and associated signaling pathways that control normal breast epithelium and breast cancer. J Mammary Gland Biol Neoplasia **16:**235–245.

http://prime-pdf-watermark.prime-prod.pubfactory.com/ | 2025-02-25

21. **Institute for Laboratory Animal Research.** 2011. Guide for the care and use of laboratory animals, 8th ed. Washington (DC): National Academies Press.
22. **Lepsy CS, Guttendorf RJ, Kugler AR, Smith DE.** 2003. Effects of organic anion, organic cation, and dipeptide transport inhibitors on Cefdinir in the isolated perfused rat kidney. Antimicrob Agents Chemother **47:**689–696.
23. **Liu T, Walsh TR, Mischinger H, Rao RN, Chelvakumar P, Rubin R, Starzl TE.** 1990. A modified apparatus for dual, sterilized, isolated perfusion of the rat liver. J Invest Surg **3:**365–372.
24. **Mackie BS, Mackie LE, Bourne DJ.** 1987. Melanoma and dietary lipids. Nutr Cancer **9:**219–226.
25. **Miller LL.** 1972. History of isolated liver perfusion and some still unsolved problems, p 1–9. In: Bartosek I, Guaitani A, Mille AA, editors. Isolated liver perfusion and its applications. New York (NY): Raven.
26. **Moley JF, Gorschbloth CM, Norton JA.** 1988. Body composition changes in rats with experimental cancer cachexia: improvement with exogenous insulin. Cancer Res **48:**2784–2787.
27. **National Research Council.** 1995. Nutrient requirements of laboratory animals, p 11–79. Washington (DC): National Academies Press.
28. **Ontell SJ, Colella MS, Horowitz T.** 1988. Applications of isolated perfused rat liver in transplantation research. J Invest Surg **1:**25–27.
29. **Reiter RJ.** 1991. Melatonin: the chemical expression of darkness. Mol Cell Endocrinol **79:**C153–C158.
30. **Reppert SM, Weaver DR.** 2002. Coordination of circadian timing in mammals. Nature **418:**935–941.
31. **Reyes N, Reyes I, Tiwari R.** 2004. Effect of linoleic acid on proliferation and gene expression in the breast cancer cell line T47D. Cancer Lett **209:**25–35.
32. **Ross BD.** 1972. Perfusion techniques in biochemistry, p 8–99. Oxford (UK): Clarendon Press.
33. **Ruderman NB, Houghton CRS, Hems R.** 1971. Evaluation of the isolated perfused rat quarter for the study of muscle metabolism. Biochem J **124:**639–651.
34. **Simopoulos AP, Robinson J. 1998.** The omega plan, p 5. New York (NY): Harper Collins.
35. **Sauer LA, Dauchy RT.** 1988. Identification of linoleic and arachidonic acids as the factors in hyperlipemic blood that increases [^{3}H] thymidine incorporation in hepatoma 7288CTC perfused in situ. Cancer Res **48:**3106–3111.
36. **Sauer LA, Dauchy RT.** 1994. Lactate release and uptake in hepatoma 7288CTC perfused in situ with L-[(U)-^{14}C]lactate or D-[(U)-^{14}C]glucose. Metabolism **43:**1488–1497.
37. **Sauer LA, Dauchy RT, Blask DE.** 2001. Melatonin inhibits fatty acid transport in inguinal fat pads of hepatoma 7288CTC-bearing and normal Buffalo rats via receptor-mediated signal transduction. Life Sci **68:**2835–2844.
38. **Sauer LA, Dauchy RT, Blask DE, Armstrong BJ, Scalici S.** 1999. 13-Hydroxyoctadienoic acid is the mitogenic signal for linoleic acid-dependent growth in rat hepatoma 7288ctc in vivo. Cancer Res **59:**4688–4692.
39. **Sauer LA, Nagel WO, Dauchy RT, Miceli LA, Austin JE.** 1986. Stimulation of tumor growth in adult rats in vivo during an acute fast. Cancer Res **46:**3469–3475.
40. **Sauer LA, Stayman JW 3rd, Dauchy RT.** 1982. Amino acid, glucose, and lactic acid utilization in vivo by rat tumors. Cancer Res **42:**4090–4097.
41. **Taft DR.** 2004. The isolated perfused rat kidney model: a useful tool for drug discovery and development. Curr Drug Discov Technol **1:**97–111.
42. **Wicha MS, Liotta LA, Kidwell WR.** 1979. Effects of free fatty acids on the growth of normal and neoplastic rat mammary epithelial cells. Cancer Res **39:**426–435.

http://prime-pdf-watermark.prime-prod.pubfactory.com/ | 2025-02-25